

Article

Insights to Achieve a Better Control of Silicon-Aluminum Ratio and ZSM-5 Zeolite Crystal Morphology through the Assistance of Biomass

Alessandra V. Silva ^{1,2}, Leandro S. M. Miranda ¹, Márcio Nele ², Benoit Louis ^{3,†,*} and Marcelo M. Pereira ^{1,†,*}

¹ Instituto de Química, Universidade Federal do Rio de Janeiro, Av. Athos da Silveira Ramos 149, CT Bloco A, Cidade Universitária, 21941-909 Rio de Janeiro, Brazil; alessandra@eq.ufrj.br (A.V.S.); leandrosoter@iq.ufrj.br (L.S.M.M.)

² Universidade Federal do Rio de Janeiro, Escola de Química Av. Athos da Silveira Ramos 149, CT Bloco E, Cidade Universitária, 21941-909 Rio de Janeiro, Brazil; nele@eq.ufrj.br

³ Institute of Chemistry, UMR 7177, University of Strasbourg, 1 rue Blaise Pascal F-67000 Strasbourg Cedex, France

* Correspondence: blouis@unistra.fr (B.L.); maciel@iq.ufrj.br (M.M.P.); Tel.: +33-3-6885-1344 (B.L.); +55-21-3938-7240 (M.M.P.)

† These authors contributed equally to this work.

Academic Editors: Andreas Martin and Keith Hohn

Received: 29 October 2015; Accepted: 14 February 2016; Published: 18 February 2016

Abstract: The present study attempts to provide insights for both the chemical composition (Si/Al) and the crystal morphology of ZSM-5 zeolites while using biomass template compounds in the synthesis. The solution containing biomass-derivative compounds was obtained after treating biomass in a sodium hydroxide aqueous solution under reflux. The latter alkaline solution was used as a solvent for zeolite nuclei ingredients to form the gel phase under hydrothermal conditions (170 °C during 24, 48 or 72 h). This approach allowed for preparing MFI zeolites having a broad range of Si/Al ratio, *i.e.*, from 25 to 150. Likewise, MFI crystals with different morphologies could be obtained, being different from the pristine zeolite formed in the absence of biomass.

Keywords: ZSM-5; biomass; sugar cane; zeolite synthesis; Si/Al

1. Introduction

ZSM-5 zeolite, discovered by Mobil Company, is a member of commonly called “big five” zeolites and has been used in several acid-catalyzed processes. For instance, its use can lead to improved gasoline quality in fluid catalytic cracking processes [1]. Ethylene and propylene selectivity can also be improved based on ZSM-5 additives [2]. Likewise this zeolite has been successfully tested in NO_x reduction [3], glycerol conversion [3,4] and in the Methanol-To-Olefins process [5]. Barely reactive σ C–H and σ C–C bonds in saturated hydrocarbons have been activated by means of zeolite catalysts [6]. We have recently demonstrated that the first step in alkane activation occurs through the protolytic cleavage of either σ C–H or σ C–C bonds, followed by bimolecular reactions involving carbocations [7]. The product selectivity is usually strongly affected by the zeolite Si/Al ratio, especially in the chemistry involving hydrocarbons [8]. In addition, the propylene selectivity (in MTO reaction) is largely enhanced in large ZSM-5 crystals and yet by higher SAR [9].

It is therefore of prime importance to design ZSM-5 catalysts with tailored SAR, crystal size, morphology and texture since these parameters play an important role in several types of

acid-catalyzed reactions. In addition, it is preferable to control these properties via a one-pot synthesis, thus avoiding sequential post-treatments.

Living organisms such as shells and corals commonly use self-assembly processes involving inorganic and organic moieties [10]. Moreover, the origin of life itself could be related to an interaction between silicon and aluminum compounds and organic molecules [11,12]. As a consequence, research combining biomass-derived compounds in alumino-silicate preparation, particularly the ones involving long synthesis duration and the formation of metastable species has great potential. Indeed, zeolites are metastable materials prepared either with an assistance of organic templates or by seed addition [13]. A clear effect between the template size and the zeolite pore architecture remains rather difficult to demonstrate. Crystal size and morphology are largely affected by the self-assembly process involved during crystal growth. In zeolite synthesis, meta-stable intermediate structures are produced, being themselves affected by the presence of different ingredients and especially the presence of organic co-components, in analogy to the aforementioned natural processes.

The use of sugar cane biomass (bagasse) in the preparation of ZSM-5 zeolite was already reported by our group [14]. This procedure greatly affected the morphology of ZSM-5 crystals, resulting in sizes between 50–100 nm. In contrast, SAR values were not greatly affected and remained in the 20–30 range, similar to the zeolite synthesized in the absence of biomass residues. It is important to highlight that small ZSM-5 crystals increased both alkane cracking activity and selectivity toward propylene and ethylene compared with large crystals [14]. This simple and inexpensive method was also applied to the preparation of γ -alumina and resulted both in surface area and pore volume increases of up to 2.5-fold and 1.5-fold, respectively, when compared to alumina preparation in the absence of biomass [15]. Furthermore, mesopores in the 2–10 nm range were produced. HRTEM measurements showed that the presence of biomass enhanced the the formation of pores by interconnection of (002) and (1-11) planes. However, no improvement in alumina textural properties prepared in the presence of a solution containing biomass-extracted compounds could be observed. These results suggest that biomass or biomass-derived components formed under *in-situ* synthesis conditions induce changes (minor or major) in the self-assembly process. We would like to stress that biomass introduction itself or a solution containing biomass-extracted compounds for preparing an inorganic material is, so far, a case-by-case phenomenon, rather than a general and well established cause-effect principle. Hence, so far catalytic properties can barely be understood '*a priori*'. Herein the effect of biomass derived-compounds, obtained by prior alkaline sugar-cane bagasse hydrolysis, was evaluated in ZSM-5 zeolite preparations.

2. Results and Discussion

In order to investigate whether the alkaline hydrolyzate from sugar-cane bagasse has an influence on the chemical composition or crystal size/morphology of ZSM-5 zeolite when added as a co-component in its synthesis, we performed the following steps:

- i Select a reliable standard preparation based on the International Zeolite Association to obtain a high Al-containing ZSM-5 zeolite [16].
- ii Repeat this procedure in the presence of biomass-derived compounds extracted by alkaline hydrolysis treatment of biomass residues.
- iii Characterize the as-prepared zeolites in terms of textural properties, SAR, microstructure, crystallinity and catalytic activity in the *n*-hexane cracking reaction.

The Leuven group has recently shown by ^{27}Al - ^1H REDOR NMR of precursor gel species that TPA^+ cations were readily incorporated at early stages, in their final configuration, in the MFI aluminosilicate (SAR = 50) [17]. This is in agreement with earlier proposed MFI self-assembly pathways [18–20].

In order to assess any effect related to the biomass presence, we have performed preliminary experiments: zeolite synthesis without fiber addition (reference materials), and analysis of hydrolyzate composition as well as fiber compositions before and after alkaline treatment. Table 1 describes both

the yield of mass loss from the bagasse, as well as the yield of the extraction. As expected, the mass loss observed after the more concentrated alkaline treatment (0.5 mol/L) is the highest. Likewise, the yield of extracted products remains the highest too (Table 1). According to former reports [21], an alkaline hydrolysis of sugar cane bagasse yielded mainly molecules from the hydrolysis of lignin, especially cinnamic acid derivatives such as coumaric and ferulic acids. The direct injection of crude hydrolyzate into a mass spectrometer equipped with an electron spray ionization source showed the main signals (M-H⁺) corresponding to the aforementioned acids. In parallel, the quantification of pentoses and hexoses by chromatography confirmed the absence of these carbohydrates in the hydrolyzate. However, partial hydrolysis or decomposition of these polymers cannot be completely ruled out but a more detailed analysis of this solution is not within the scope of this report.

Table 1. Analysis of alkaline hydrolysis solution of sugar cane bagasse.

Biomass Treatment (mol/L NaOH)	Yield of Bagasse Mass Loss (%) ^a	Extract Yield (%) ^b
0.1	14	8
0.5	52	45

^a [(initial bagasse mass – recovery bagasse mass)/initial bagasse mass] × 100; ^b [mass extract/(initial bagasse mass – recovery bagasse mass)] × 100.

With this alkaline hydrolyzate in hand, we then proceeded to evaluate its influence in the synthesis of ZSM-5 when used as a solvent. The ZSM-5 zeolite preparation in the absence of hydrolyzate led to a highly crystalline zeolite, as shown in Table 2. The chemical analysis of SAR (including both non- and framework aluminum) showed an increase ranging from 24 to 37 for crystallization times of 24 to 48 h. SAR did not change further after 72 h of synthesis. This slight increase in SAR with ageing time is regularly observed for ZSM-5 synthesis as siliceous species can be continuously incorporated in the framework [20]. However higher intensities in XRD diffraction lines for 48 h were observed compared to the ones detected after a 24 h material synthesis (roughly a 15% raise based on the two theta = 23° reflexion). An optimum synthesis time has therefore to be found to guarantee a high crystallinity.

Table 2. ZSM-5 textural and structural properties.

Catalysts	SAR XRF	Micro cm ³ ·g ⁻¹	Meso cm ³ ·g ⁻¹	Rel. XRD	Particle Size (μm)
Ref. [1]	27	0.15	0.025	100	1-3
Ref. [2]	26	n.d.	n.d.	100	1-3
Ref. [3]	37	n.d.	n.d.	100	1-3
ZSM-5 A(24)	107	0.17	0.018	88	1-3
ZSM-5 B(48)	143	0.16	0.017	98	1-4
ZSM-5 C(72)	153	0.16	0.018	97	6-10
ZSM-5 D(24)	24	0.16	0.017	93	3-7
ZSM-5 E(48)	81/98 *	0.16	0.017	106	7-8
ZSM-5 F(72)	119	0.17	0.017	88	7-11

* These two zeolites were synthesized twice to assess the reproducibility of the protocol.

The textural properties of as-prepared ZSM-5 zeolites as a function of both the type of biomass derivative-solution and ageing time are presented in Table 2. The pristine MFI zeolite pattern, prepared without biomass-derivate compounds (Refs. [1,2]) were included. Firstly, it is important to highlight that all materials exhibited all the characteristic diffraction lines of a unique MFI structure (Figure 1). All zeolites were compared with (Ref. [2]) to estimate the relative crystallinity and exhibited high crystallinities, above 87%. Additional DRX experiment of ZSM-5 E (48) and a commercial ZSM-5 sample (results not shown) were performed and both zeolites showed similar crystallinity, therefore we can assure that the relative crystallinity values detailed in Table 2 for the zeolite samples

prepared with and without the biomass-derivatives assistance are comparable to those of conventional prepared zeolites.

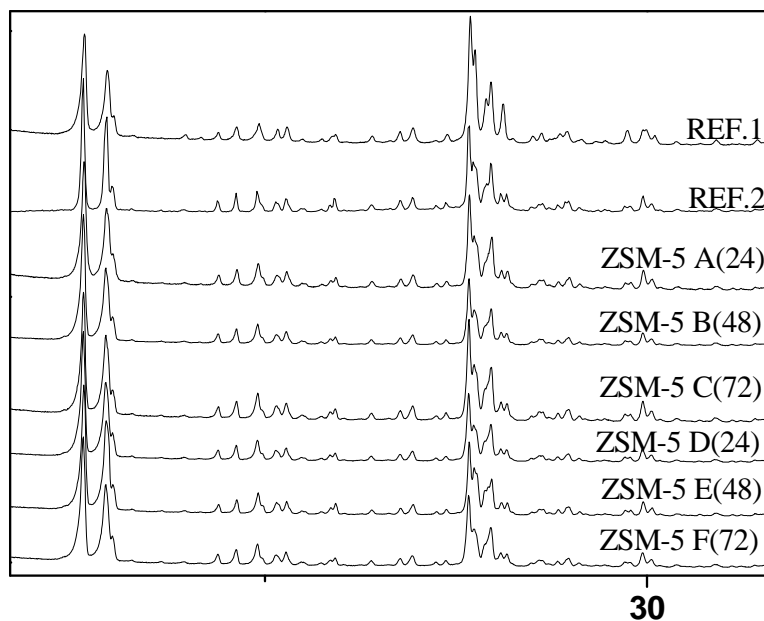


Figure 1. Diffraction patterns for the different zeolites: Ref. [1] series and Ref. [2]. series Zeolite synthesized for 24 h; NaOH 0.1 mol/L (ZSM-5 A(24)); for 48 h; NaOH 0.1 mol/L (ZSM-5 B(48)); for 72 h NaOH 0.1 mol/L (ZSM-5 C(72)); for 24 h; NaOH 0.5 mol/L (ZSM-5 D(24)); for 48 h; NaOH 0.5 mol/L (ZSM-5 E(48)); for 72 h; NaOH 0.5 mol/L (ZSM-5 F(72)).

Secondly, ZSM-5 properties were discussed in terms of SAR, textural property, crystal size, and morphology (Table 2). As observed for ZSM-5 reference materials (prepared in the absence of biomass), longer ageing times led to higher SAR values. However, a broad range of SAR was observed and yet the extract obtained at 0.1 mol/L of NaOH resulted in higher values compared to those reached at 0.5 mol/L of NaOH.

The SAR based on the bulk composition was remarkably affected and values in the range of 25 to 150 were measured. Microporosities and mesoporosities are rather similar for all zeolites in line with literature data [22,23]. For the sake of clarity, a parent ZSM-5 was characterized by the nitrogen adsorption/desorption technique and similar microporous volumes were measured. ZSM-5 prepared in the presence of biomass derived-compounds exhibited a slightly lower mesoporous volume compared to its parent ZSM-5 counterpart. The ZSM-5 structure is orthorhombic (Pnma space group) when high thermal treatment is conducted [24,25], usually resulting in prismatic crystal formation [26] as observed for reference zeolites (Figure 2). The standard method used for preparing ZSM-5 zeolite resulted in 1–3 μm range crystal size with no changes in morphology with ageing time. In contrast, both morphology and particle size were affected by the presence of biomass derived-compounds. The extract obtained at 0.1 mol/L led to regular (size and type) ZSM-5 crystals at an ageing time of 24 h. A further raise in ageing time to 48 h led to the formation of crystals having the same size, but extremely different in terms of morphology that was constructed by an assembly of elongated French-fries having 100 nm in width. At longer ageing times, larger crystals were formed, exhibiting again a conventional morphology. In contrast to ZSM-5 A(24) sample, ZSM-5 C(72) sample exhibits sharper crystal outer rim and appears to be more faceted. While studying the influence of alkali cation nature and gel ionic strength, Petrik *et al.* were able to synthesize MFI zeolites with significant changes in morphology and drawn the conclusion that minor alterations of the composition may lead to major changes in the crystal growth [27].

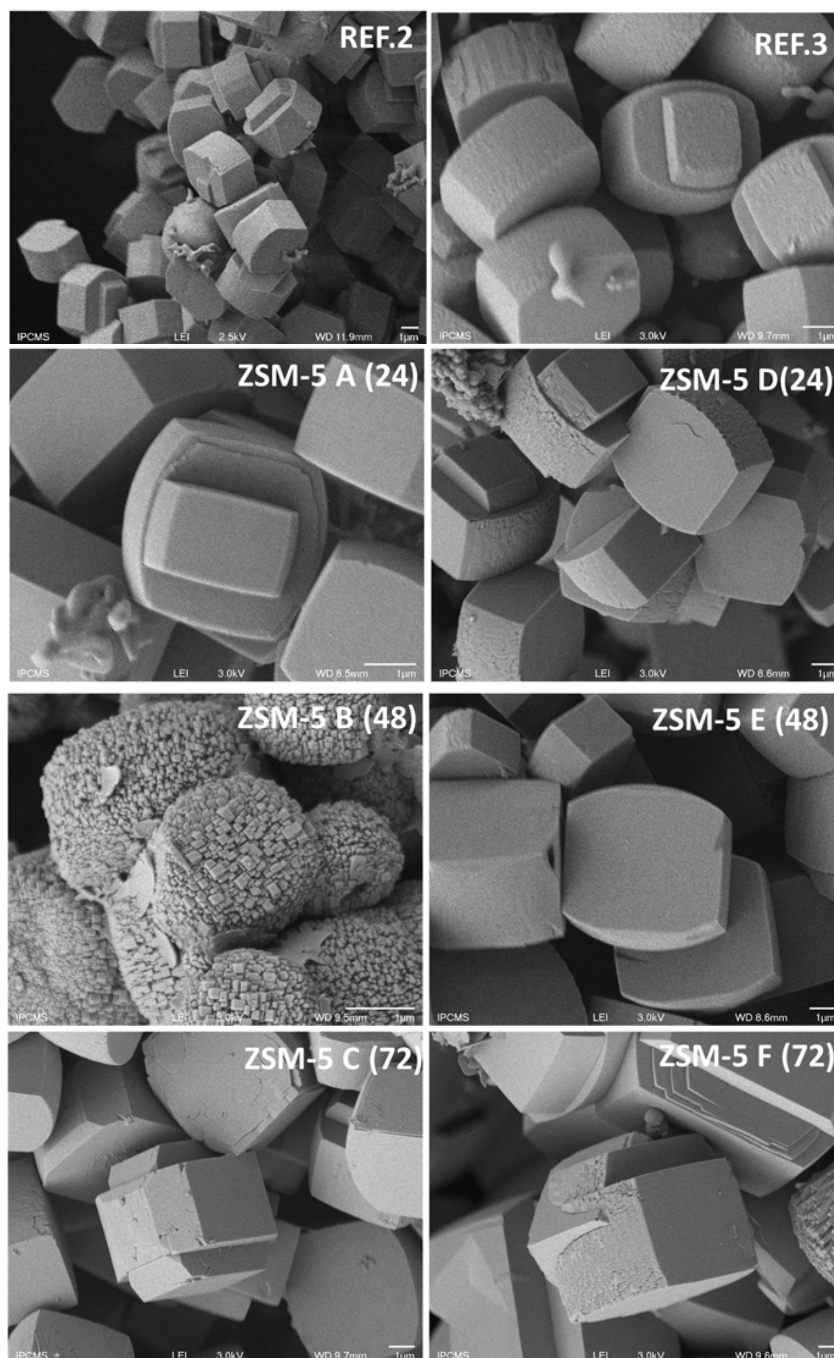


Figure 2. SEM images (1 μm scale-bar) of zeolites synthesized for different durations.

In the ZSM-5 zeolite synthesis with biomass extract (obtained by hydrolysis in NaOH 0.5 mol/L, aged during 24 h, ZSM-5 D), conventional MFI coffin-shape crystals were formed, being larger than those observed without biomass-derived compounds (Refs. [1,2]). After extending the ageing time to 48 h (ZSM-5 E(48)) a further increase in the crystal size was observed, but the common shape for ZSM-5 crystals was still maintained. It seems however that the surface roughness diminished for ZSM-5 E(48) which may indicate a higher crystallinity. This assumption is in line with XRD data (Table 2). In contrast, after an ageing time of 72 h, ZSM-5 F(72) exhibits a similar morphology to ZSM-5 D(24) but with a high level of intergrowth. A peculiar crystal aggregation mechanism seems to occur, resulting in extensive twinning observed for longer synthesis durations. This might be due to dissolution/recrystallization phenomena, involving peculiar self-assembly processes during the

crystal growth. Since zeolites are metastable materials, it is possible to shift from one structure to another one [28], or to crystallize in various morphologies by a simple change in the synthesis duration. This phenomenon was already observed for SiC substrate self-reconstruction into zeolites [29,30].

The cracking of *n*-hexane or so-called alpha test [31] is an useful tool for ranking the catalytic activity of acidic zeolites since catalytic activity is related to both the number and type of acid sites and also to the morphology and crystal organization. The *n*-hexane activity is indeed lower compared to the commercial ZSM-5 [22] zeolite and remains similar to deactivated ZSM-5 [32], including the reference ZSM-5 (Ref. [1]). The ZSM-5 zeolite prepared with an extract of biomass (0.1 mol/L), samples A, B and C, exhibited similar relative crystallinity and textural properties. The rate of hexane consumption for the zeolite obtained after an ageing time of 72 h, was two-fold higher than the one achieved after 24 h ageing (Table 3). In contrast, SAR was 1.5-fold higher in the former, *i.e.* probably resulting in a lower quantity of Brønsted acid sites. ZSM-5 C(72) exhibits a high degree of twinning which led to higher exposure of straight channel pore openings. Hence, this may render easier the access to active sites and therefore speed up the cracking rate. In contrast, only minor changes could be observed in the selectivity toward propylene for all samples. Since the aim of this manuscript was to evaluate the acid properties of those zeolites the lower conversion regime was adopted therefore sequential reactions by re-conversion of primary and secondary products of *n*-hexane were avoided. As a consequence a lower effect on selectivity was observed and yet heavier compounds than *n*-C₆ were severely suppressed. For instance similar propane/propene ratios (as presented in Table 2) varied between 0.34–0.39 and yet the coke amount (not shown) varies in the range 0.3–0.4 wt % in spent ZSM-5.

Table 3. Data obtained in the *n*-hexane catalytic cracking reaction.

Catalyst	Conversion	Rate <i>n</i> C6 *	C3=	Propane/Propylene
Ref. [1]	2.1	0.78	0.26	0.35
A	1.8	0.38	0.26	0.35
B	2.7	0.57	0.28	0.39
C	3.5	0.71	0.32	0.37
D	2.9	0.60	0.31	0.36
E	3.4	0.71	0.33	0.36
F	2.1	0.43	0.28	0.34

* mmol·g·cat⁻¹·min⁻¹.

Regarding, ZSM-5 D(24) to F(72) catalysts, it appears that the highest rate of *n*-hexane cracking was achieved for ZSM-5 E(48), that exhibits the highest crystallinity. In contrast, the alkane cracking rate was the lowest for ZSM-5 F(72). The latter zeolite seems to be built by different aggregation mechanism(s), since its surface remains rather heterogeneous. The self-assembly of smaller building blocks (like slabs) may generate a higher surface permeability in those smaller sub-units [33,34]. According to Karger *et al.*, these surface barriers may induce a higher resistance for the molecules to enter inside the pores in smaller crystals [33], thus reducing the reaction rate.

These results clearly demonstrate that the ZSM-5 properties (SAR, crystal size, crystallization, and morphology) are remarkably affected by the presence biomass-derived compounds that were obtained by alkaline hydrolysis of sugar-cane bagasse. These effects could be rationalized in terms of a direct interaction of the compounds present in the hydrolyzate and aluminate/silicate species. Besides, the crystal nucleus surface affects the self-assembly process and therefore the crystal growth. Moreover, an interaction between biomass derived-compounds and inorganic precursors is occurring during the ageing time (after the crystals are readily formed), probably via a continuous process of redissolution/recrystallization at longer synthesis times [35]. We highlight that this process is barely observed during ZSM-5 synthesis in the absence of biomass-derived compounds and only a moderate increase in SAR was achieved during ageing time. As aluminate species were already dissolved in the gel, the incorporation of silicates is favored by a sequential process. It is therefore expected that longer ageing times result in higher SAR values, as observed from Refs. [1–3]. The process of

raising SAR can be related to both an introduction of silicates and alternatively to aluminum removal (as extra-framework aluminum species).

The molecular and supramolecular events taking place during zeolite synthesis are very complex and not yet fully understood. By taking as model compounds the acids detected by ESI-MS/MS, we can hypothesize that these phenolic acids, as well as other components present in the hydrolyzate such as carbohydrates (probably polysaccharides), may possibly complex aluminum and/or silicon. Indeed, many complexes of phenolates, cinnamic acid derivatives with aluminum were readily reported in literature [36,37]. In addition, those complexes may further react with carbohydrates. In the frame of zeolite synthesis, these complexes may interfere in the crystal organization synthesizing modulating the incorporation and/or removal of T-elements (T: Al or Si) from the framework. Finally, we believe that after consolidation and understanding of all events involved in zeolite preparation with the assistance of biomass-derivate, this approach could work as a powerful tool for tailoring zeolite properties.

3. Experimental Section

Untreated sugar cane bagasse (20 g) was ground and particles in the 20–80 mesh size range were selected. The bagasse was washed using de-ionized water at 50 °C, filtered and dried in a Buchner funnel. This procedure was repeated eight times. Then, the bagasse was used in alkaline hydrolysis conditions, suspended in a 20 mL NaOH solution (either 0.1 or 0.5 mol/L). These alkaline treatments of biomass residues were conducted for 1 h under reflux. Afterwards, the suspension was filtered to remove unreacted fibers and diluted to 100 mL. Thirty mL of this solution was used for the zeolite synthesis. Prior to the ZSM-5 zeolite preparation, the pH of the biomass derived-compound solution obtained after hydrolysis with 0.1 and 0.5 mol/L of NaOH was adjusted to 12 by adding 0.1 and 0.5 mol/L HCl solution, respectively. Then 0.08 g NaAlO₂ and 8 mL TPAOH (20 wt % in water) were added to this solution under vigorous stirring. Likewise, 0.76 g NaCl were added, prior to a dilution in 30 mL distilled water. Finally, 6 mL TEOS were added dropwise. The solution was allowed to age for 1h at room temperature and then autoclaved at 170 °C during 24, 48 or 72 h. 1.2–1.3 g of ZSM-5 zeolites were obtained after Millipore membrane filtration. The zeolite was dried at 120 °C overnight and then calcined at 600 °C.

X-Ray diffraction (XRD) was performed using an Ultima IV diffractometer (Rigaku, Tokyo, Japan, Cu K_α = 0.1542 nm) at a scanning rate of 0.02 s⁻¹ in 2θ ranges from 5 to 80°. A fixed power source was used (40 kV, 20 mA). The relative crystallinity of ZSM-5 phase was determined by the area of the peaks at 2θ 23.1° to 24.1°. The crystallinity was arbitrarily set to 100% for pristine reference zeolites (1 and 2) exhibiting the same crystallinity. Scanning electron microscopy (SEM) micrographs were acquired on a FEG 6700F microscope (JEOL, Tokyo, Japan) working at a 9 kV accelerating voltage. X-Ray fluorescence was carried out to estimate the SAR using a Magic X instrument (Phillips, Almalo, The Netherlands). The textural properties were evaluated using *n*-hexane adsorption as presented elsewhere [38]. ZSM-5 samples were placed in an 85 μL crucible and analyzed by an Iris TG 209 F1 thermal analyzer (Netzsch, Selb, Germany). Firstly, the sample was pre-treated to remove water (this step comprises heating in N₂ flow (60 mL·min⁻¹) from room temperature to 600 °C at 10°·min⁻¹ plus 30 min kept at final temperature. Secondly, the sample was cooled to 160 °C. Finally, *n*-hexane adsorption was carried out continuously, followed by weight variation, during cooling from 160 °C to 40 °C at 4°·min⁻¹ under a flow of 8% of *n*-hexane in N₂. Silicon-to-aluminum ratios were determined by XRF.

The catalytic cracking of *n*-hexane (99.89% pure, water 0.005 wt % no volatile residue 0.001% wt/wt from (VETEC/ Sigma-Aldrich Chemistry Ltda., St. Louis, MO, USA) was conducted in a high-throughput unit. Eight reactors in parallel (187 mm in length and 6 mm of internal diameter) made of quartz, with the catalyst localized 90 mm below the top of the reactor, were placed in the middle part of an oven (400 mm external diameter). The temperature was measured by means of a thermocouple located in the center of each reactor and differed less than two degrees between the reactors. All experiments were performed at atmospheric pressure in a continuous down flow fixed-bed

micro-reactor. Prior to catalyst evaluation, all the materials were simultaneously heated in nitrogen from room temperature to the reaction temperature (500 or 600 °C) at 10°/min. Then, nitrogen was fed through a saturator containing *n*-hexane at 20 °C to the reactors. This procedure ensured a 60 mL/min of 11% *v/v* *n*-hexane flow in nitrogen. Since the catalysts were evaluated sequentially, the activation time (at the final temperature) is different for each reactor. This difference did not affect activity and selectivity results. A typical run was carried out with 0.1 to 0.03 g of catalyst (the amounts of catalyst were adjusted in order to provide iso conversion conditions). Reaction products were analyzed on-line after three different times on stream (3, 17, and 32 min) by gas chromatography using a GC-2010 apparatus (Shimadzu, Tokyo, Japan) equipped with a Chrompack KCl/Al₂O₃ column operated under isothermal conditions (303 K) and nitrogen flow (2 mL/min). Catalytic activity and selectivity were estimated as an average of results obtained after 17 and 32 min on-stream. These values differed by less than 10% and 2% for activity and selectivity, respectively (each catalyst was analyzed three times). Propylene selectivity was estimated as percentage in *wt/wt* divided by the total conversion in *wt/wt* and the alkene/alkane ration was estimated as the total alkenes formation in *wt/wt* % referred to total alkane formation in *wt/wt* %. The catalysts showed a moderated to low deactivation (the catalytic activity at 3 min on time on stream differs less than 15%, when compared to the one measured after 32 min).

4. Conclusions

Pure ZSM-5 zeolite phases were successfully synthesized in the presence of alkaline solutions containing biomass-derived compounds. The presence of these compounds remarkably affected the silicon/aluminum ratio varying from 25 to 150, compared with SAR obtained in the absence of biomass-derived compounds (from 27 to 37). Moreover ZSM-5 crystals with different crystal sizes as well as peculiar morphologies were obtained.

The solutions containing biomass-derived compounds were obtained by alkaline hydrolysis treatment under reflux of second-generation biomass; therefore this procedure can be easily implemented in regular ZSM-5 synthesis and further extended to other zeolite preparation. Similar cracking activities and selectivities were achieved over as-prepared biomass-derived zeolites with respect to parent ZSM-5 zeolites.

Acknowledgments: Alessandra V. Silva is grateful to the Programa de Pós Graduação em Tecnologia de Processos Químicos e Bioquímicos da Escola de Química.

Author Contributions: MMP and BL have developed this research area. BL proposed the concept and initiated the zeolite syntheses at the University of Strasbourg. MMP shared his experience in biomass valorization and wrote the main part of the paper. AVS performed the ZSM-5 zeolite preparations and most of the characterizations; LSMM and MN performed the thorough characterization of biomass components by LC-MS-MS techniques.

Conflicts of Interest: The authors declare no conflict of interest.

References

1. Donnelly, S.P.; Mizrahi, S.; Sparrell, P.T.; Huss, A.J.; Schipper, P.H.; Herbst, J.A. How ZSM-5 works in FCC. In Proceedings of ACS Meeting, New Orleans, LA, USA, 30 August–4 September 1987; 1987; pp. 621–626.
2. Buchanan, J.S. The chemistry of olefins production by ZSM-5 addition to catalytic cracking units. *Catal. Today* **2000**, *55*, 207–212. [[CrossRef](#)]
3. Burch, R.; Scire, S. Selective catalytic reduction of nitric oxide with ethane and methane on some metal exchanged ZSM-5 zeolites. *Appl. Catal. B* **1994**, *3*, 295–318. [[CrossRef](#)]
4. Zakaria, Z.Y.; Linnekoski, J.; Amin, N.A.S. Catalyst screening for conversion of glycerol to light olefins. *Chem. Eng. J.* **2012**, *207–208*, 803–813. [[CrossRef](#)]
5. Chang, C.D. Methanol conversion to light olefins. *Catal. Rev.* **1984**, *26*, 323–345.
6. Sassi, A.; Sommer, J. Isomerization and cracking reactions of branched octanes on sulfated zirconia. *Appl. Catal. A* **1999**, *188*, 155–162. [[CrossRef](#)]

7. Louis, B.; Pereira, M.M.; Santos, F.M.; Esteves, P.M.; Sommer, J. Alkane activation over acidic zeolites: The first step. *Chem. Eur. J.* **2010**, *16*, 573–576. [[CrossRef](#)] [[PubMed](#)]
8. Olah, G.A.; Molnar, A. *Hydrocarbon Chemistry*, 2nd ed.; Wiley Interscience: New York, NY, USA, 2003.
9. Lønstad Bleken, F.; Chavan, S.; Olsbye, U.; Boltz, M.; Ocampo, F.; Louis, B. Conversion of Methanol into light olefins over ZSM-5 zeolite: Strategy to enhance propene selectivity. *Appl. Catal. A* **2012**, *447–448*, 178–185.
10. Mann, S. The chemistry of form. *Angew. Chem. Int. Ed.* **2000**, *39*, 3392–3406. [[CrossRef](#)]
11. Feuillie, C.; Sverjensky, D.A.; Hazen, R.M. Attachment of ribonucleotides on α -alumina as a function of pH, ionic strength, and surface loading. *Langmuir* **2015**, *31*, 240–248. [[CrossRef](#)] [[PubMed](#)]
12. Fraser, D.G.; Fitz, D.; Jakschitz, T.; Rode, B.M. Selective adsorption and chiral amplification of amino acids in vermiculite clay-implications for the origin of biochirality. *Phys. Chem. Chem. Phys.* **2011**, *13*, 831–838. [[CrossRef](#)] [[PubMed](#)]
13. Cundy, C.S.; Cox, P.A. The hydrothermal synthesis of zeolites: Precursors, intermediates and reaction mechanism. *Microporous Mesoporous Mater.* **2005**, *82*, 1–78. [[CrossRef](#)]
14. Ocampo, F.; Cunha, J.A.; de Lima Santos, M.R.; Tessonnier, J.P.; Pereira, M.M.; Louis, B. Synthesis of zeolite crystals with unusual morphology: Application in acid catalysis. *Appl. Catal. A* **2010**, *390*, 102–109. [[CrossRef](#)]
15. Cardoso, C.S.; Licea, Y.E.; Huang, X.; Willinger, M.; Louis, B.; Pereira, M.M. Improving textural properties of γ -alumina by using second generation biomass in conventional hydrothermal method. *Microporous Mesoporous Mater.* **2015**, *207*, 134–141. [[CrossRef](#)]
16. Chou, Y.H.; Cundy, C.S.; Garforth, A.A.; Zholobenko, V.L. Mesoporous ZSM-5 catalysts: Preparation, characterisation and catalytic properties. Part I: Comparison of different synthesis routes. *Microporous Mesoporous Mater.* **2006**, *89*, 78–87. [[CrossRef](#)]
17. Magusin, P.C.M.M.; Zorin, V.E.; Aerts, A.; Houssin, C.J.Y.; Yakovlev, A.L.; Kirschhock, C.E.A.; Martens, J.A.; van Santen, R.A. Template-aluminosilicate structures at the early stages of zeolite ZSM-5 formation. A combined preparative, solid-state NMR, and computational study. *J. Phys. Chem. B* **2005**, *109*, 22767–22774. [[CrossRef](#)] [[PubMed](#)]
18. Burkett, S.L.; Davis, M.E. Mechanism of structure direction in the synthesis of Si-ZSM-5: An investigation by intermolecular ^1H - ^{29}Si CP MAS NMR. *J. Phys. Chem.* **1994**, *98*, 4647–4653. [[CrossRef](#)]
19. Larsen, S.C. Nanocrystalline zeolites and zeolite structures: Synthesis, characterization, and applications. *J. Phys. Chem. C* **2007**, *111*, 18464–18474. [[CrossRef](#)]
20. Cundy, C.S.; Cox, P.A. The hydrothermal synthesis of zeolites: History and development from the earliest days to the present time. *Chem. Rev.* **2003**, *103*, 663–702. [[CrossRef](#)] [[PubMed](#)]
21. Ou, S.Y.; Luo, Y.L.; Huang, C.H.; Jackson, M. Production of coumaric acid from sugarcane bagasse. *Innovative Food Sci. Emerg. Technol.* **2009**, *10*, 253–259. [[CrossRef](#)]
22. Maia, A.J.; Louis, B.; Lam, Y.L.; Pereira, M.M. Ni-ZSM-5 catalysts: detailed characterization of metal sites for proper catalyst design. *J. Catal.* **2010**, *269*, 103–109. [[CrossRef](#)]
23. Xue, T.; Chen, L.; Wang, Y.M.; He, M.-Y. Seed-induced synthesis of mesoporous ZSM-5 aggregates using tetrapropylammonium hydroxide as single template. *Microporous Mesoporous Mater.* **2012**, *156*, 97–105. [[CrossRef](#)]
24. Brandenberger, S.; Kröcher, O.; Casapu, M.; Tissler, A.; Althoff, R. Hydrothermal deactivation of Fe-ZSM-5 catalysts for the selective catalytic reduction of NO with NH_3 . *Appl. Catal. B* **2011**, *101*, 649–659. [[CrossRef](#)]
25. Le van Mao, R.; Le, S.T.; Ohayon, D.; Caillibot, F.; Gelebart, L.; Denes, G. Modification of the micropore characteristics of the desilicated ZSM-5 zeolite by thermal treatment. *Zeolites* **1997**, *19*, 270–278. [[CrossRef](#)]
26. Louis, B.; Rocha, C.C.; Balanqueux, A.; Boltz, M.; Losch, P.; Bernardon, C.; Bénétiau, V.; Pale, P.; Pereira, M.M. Unraveling the importance of zeolite crystal morphology. *L'Actualité Chim.* **2015**, *393–394*, 108–111.
27. Petrik, L. The influence of cation, anion and water content on the rate of formation and pore size distribution of zeolite ZSM-5. *S. Afr. J. Sci.* **2009**, *105*, 251–257.
28. Ocampo, F.; Yun, H.; Pereira, M.M.; Tessonnier, J.P.; Louis, B. Design of MFI zeolite-based composites with hierarchical pore structure: a new generation of structured catalysts. *Cryst. Growth Des.* **2009**, *9*, 3721–3729. [[CrossRef](#)]
29. Ivanova, S.; Louis, B.; Ledoux, M.J.; Pham-Huu, C. Auto-Assembly of Nanofibrous Zeolite Crystals via Silicon Carbide Substrate Self-Transformation. *J. Am. Chem. Soc.* **2007**, *129*, 3383–3391. [[CrossRef](#)] [[PubMed](#)]
30. Losch, P.; Boltz, M.; Soukup, K.; Song, I.-H.; Yun, H.S.; Louis, B. Binderless zeolite coatings on macroporous α -SiC foams. *Microporous Mesoporous Mater.* **2014**, *188*, 99–107. [[CrossRef](#)]

31. Miale, J.N.; Chen, N.Y.; Weisz, P.B. Catalysis by crystalline aluminosilicates: Attainable catalytic cracking rate constants, and superactivity. *J. Catal.* **1966**, *6*, 278–287. [[CrossRef](#)]
32. Wallenstein, D.; Kanz, B.; Haas, A. Influence of coke deactivation and vanadium and nickel contamination on the performance of low ZSM-5 levels in fcc catalysts. *Appl. Catal. A* **2000**, *192*, 105–123. [[CrossRef](#)]
33. Tzoulaki, D.; Heinke, L.; Lim, H.; Li, J.; Olson, D.; Caro, J.; Krishna, R.; Chmelik, C.; Karger, J. Assessing Surface Permeabilities from Transient Guest Profiles in Nanoporous Host Materials. *Angew. Chem. Int. Ed.* **2009**, *48*, 3525–3528. [[CrossRef](#)] [[PubMed](#)]
34. Karwacki, L.; Kox, M.H.F.; de Winter, D.A.M.; Drury, M.R.; Meeldijk, J.D.; Stavitski, E.; Schmidt, W.; Mertens, M.; Cubillas, P.; John, N.; *et al.* Morphology-dependent zeolite intergrowth structures leading to distinct internal and outer-surface molecular diffusion barriers. *Nature Mater.* **2009**, *8*, 959–965. [[CrossRef](#)]
35. Louis, B.; Laugel, G.; Pale, P.; Pereira, M.M. Rational design of microporous and mesoporous solids for catalysis: From the molecule to the reactor. *ChemCatChem* **2011**, *3*, 1263–1272. [[CrossRef](#)]
36. Shaw, A.J.; Tsao, G.T. Isomerization of D-glucose with sodium aluminate: mechanism of the reaction. *Carbohydr. Res.* **1978**, *60*, 327–325. [[CrossRef](#)]
37. Lambert, J.B.; Lu, G.; Singer, S.R.; Kolb, V.M. Silicate complexes of sugars in aqueous solution. *J. Am. Chem. Soc.* **2004**, *126*, 9611–9625. [[CrossRef](#)] [[PubMed](#)]
38. Lowen, J.; Jonker, R. Method of analyzing microporous material. US Patent N 60/261920, 15 January 2001.



© 2016 by the authors; licensee MDPI, Basel, Switzerland. This article is an open access article distributed under the terms and conditions of the Creative Commons by Attribution (CC-BY) license (<http://creativecommons.org/licenses/by/4.0/>).